Supporting Information for

Creation of MOFs with open metal sites by partial replacement with metal ions having different coordination numbers

Yuki Harada,[a] Yuh Hijikata,[b] Shinpei Kusaka,[a] Akihiro Hori,[a] Yunsheng Ma,[a,c] and Ryotaro Matsuda[*a]

a. Department of Chemistry and Biotechnology, School of engineering, Nagoya University, Chikusa-ku, Nagoya 464-8603, Japan.

b. Department of Chemistry, Graduate School of Science and Institute of Transformative Bio-Molecules (WPI-ITbM), Nagoya University, Chikusa-ku, Nagoya 464-8602, Japan.

c. School of Chemistry and Materials Engineering, Jiangsu Key Laboratory of Advanced Functional Materials, Changshu Institute of Technology, Changshu, Jiangsu 215500, PR China.

Experimental section

Chemicals.

$Cu(BF_4)_2 \cdot 6H_2O$ and $Pd(en)(ONO_2)_2$ were purchased from Wako Pure Chemical Industries Ltd., $(NH_4)_2SiF_6$ was from Sigma-Aldrich Co., Ltd., 4,4′-bipyridine (bpy) was from Tokyo Chemical Industry and ethanol (EtOH) was from Nacalai Tesque.

Preparation of $[Cu(SiF_6)(bpy)_2]$ (SIFSIX-1-Cu).

Single crystal of **SIFSIX-1-Cu** was prepared referring to the previous reported procedures.[1] First, $Cu(BF_4)_2 \cdot 6H_2O$ (17.3 mg, 0.050 mmol) and $(NH_4)_2SiF_6$ (8.91 mg, 0.050 mmol) were dissolved in 1 mL of H_2O and stirred for 1 h. Bpy (15.6 mg, 0.10 mmol) was also dissolved in 1 mL of EtOH. Next, in the glass tube (8 mm diameter and 200 mm length), the metal solution was slowly poured to the bottom layer, 0.50 mL of mixture solvent of EtOH: H_2O=1:1 (v/v) to the middle layer, and 1.0 mL of the ligand solution to the top layer. The resultant purple square-shaped crystals were collected after a week. (Yield: 74%)

Preparation of $[Cu_{1-x}Pd_x(SiF_6)(bpy)_2]$ (SIFSIX-1-CuPd-n).

$Cu(BF_4)_2 \cdot 6H_2O$ (138 mg, 0.40 mol) and $(NH_4)_2SiF_6$ (71.3 mg, 0.40 mol) were dissolved in 10 mL of H_2O and stirred for 1 h. After that, different amounts of $Pd(en)(ONO_2)_2$ (n=3: 3.49 mg, 0.012 mol; n=5: 5.81 mg, 0.020 mol; n=10: 11.6 mg, 0.040 mol) were added into the solution and stirred again for 30 min. This metal solution and bpy (125 mg, 0.80 mol) dissolved in 10 mL of EtOH were added in the 20 mL microwave container and heated for 3 h at 100 °C under microwave irradiation. The reaction mixture was washed with 25 mL of H_2O and EtOH for 3 times. (Yield: **SIFSIX-1-CuPd-3**: 60%, **SIFSIX-1-CuPd-5**: 63%, **SIFSIX-1-CuPd-10**: 63%)
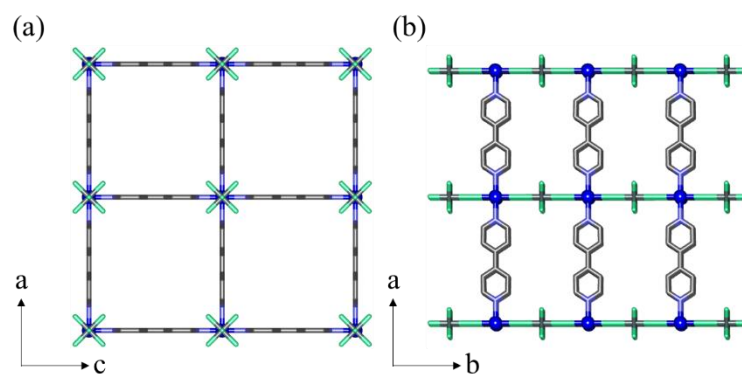
Structure.

Fig. S1 Crystal structure of **SIFSIX-1-Cu** (blue: Cu, grey: C, purple: N, black: Si, green: F). Viewing along (a) plane (010) and (b) plane (001).

Methods

Powder X-ray Diffraction (PXRD) Measurement.

All PXRD data were collected on a Rigaku MiniFlex600 operating at 40 kV/15 mA producing Cu Kα radiation (λ=1.5406 Å) at room temperature ranging from 3° to 55° with the scan rate of 1°/min.
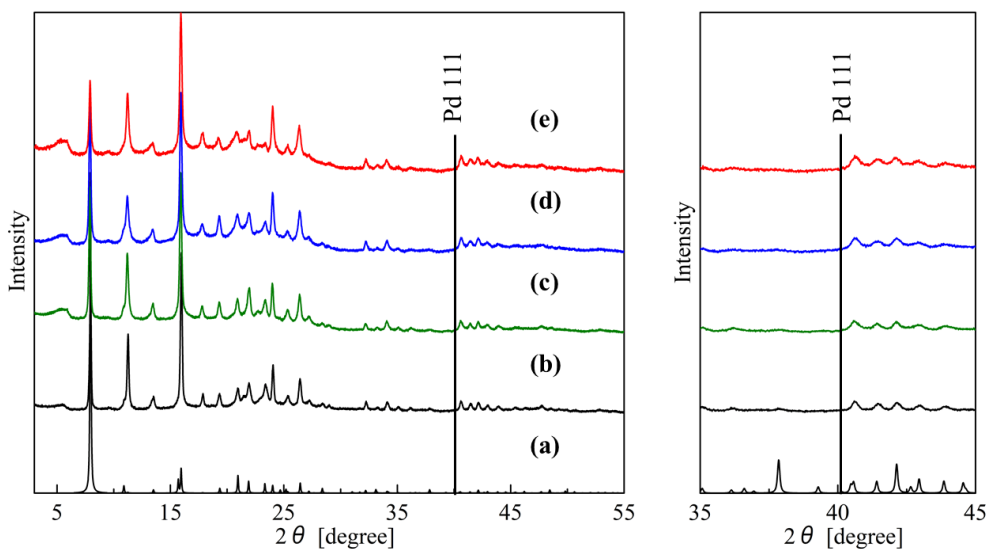

Fig. S2 PXRD patterns of (a) simulated **SIFSIX-1-Cu**, and as-synthesized (b) **SIFSIX-1-Cu**, (c) **SIFSIX-1-CuPd-3**, (d) **SIFSIX-1-CuPd-5**, (e) **SIFSIX-1-CuPd-10**. The vertical lines are the peak position of Pd face-centered cubic (fcc) structure.
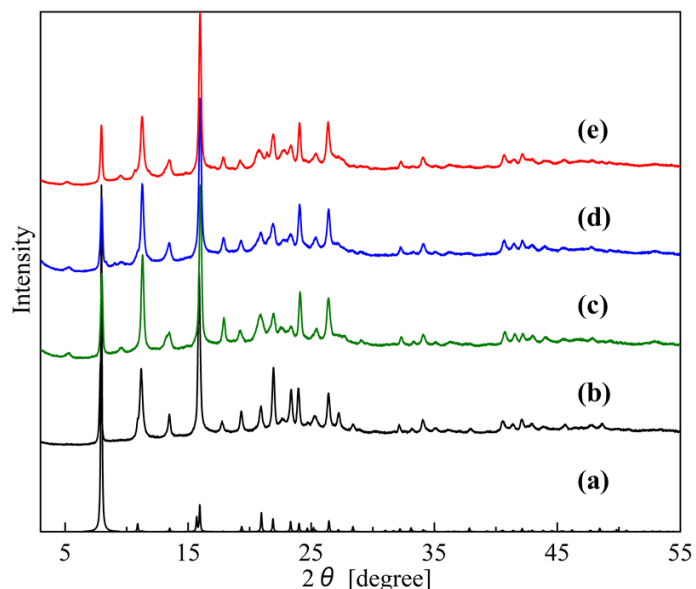

Fig. S3 PXRD patterns of (a) simulated **SIFSIX-1-Cu**, and as-synthesized (b) **SIFSIX-1-Cu**, (c) **SIFSIX-1-CuPd-3**, (d) **SIFSIX-1-CuPd-5**, (e) **SIFSIX-1-CuPd-10** which were stored under atmospheric condition for eight months.

Infrared spectroscopic (IR) measurement.

IR measurements were performed with a JEOL FT/IR 4200 spectrometer. **SIFSIX-1-Cu** and **SIFSIX-1-CuPd-n** samples were heated at 120 °C for 2 h. After the heating, IR spectra were measured from 4000 cm^{-1} to 500 cm^{-1} by attenuated total reflection (ATR) method.
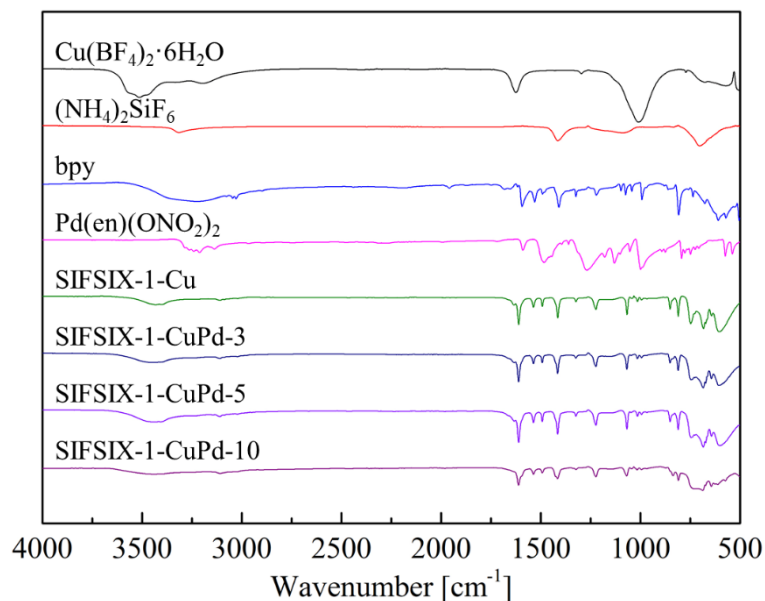

Fig. S4 IR spectra of starting materials, **SIFSIX-1-Cu**, and **SIFSIX-1-CuPd-n**.
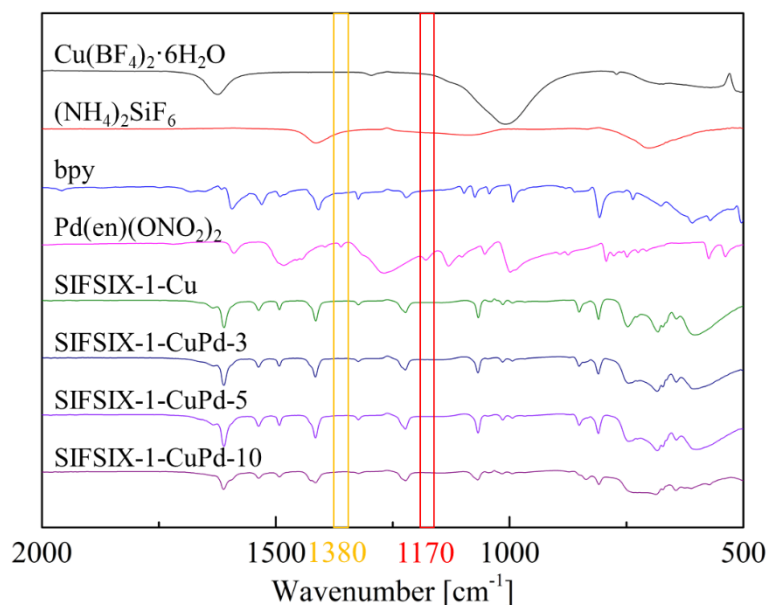

Fig. S5 Enlarged view of IR spectra of starting materials, **SIFSIX-1-Cu**, and **SIFSIX-1-CuPd-n** in 2000−500 cm^{-1}. The peaks at 1380 cm^{-1} and 1170 cm^{-1} correspond to nitrate and ethylenediamine, respectively.

Scanning Electron Microscopy (SEM) / Energy Dispersive X-ray Spectroscopy (EDX).

SEM measurements were performed with a JEOL Model JSM-7500F operating at 10 kV. The samples were heated at 120 °C in vacuum for 2 h, put on the carbon tape and coated with osmium prior to the measurements. EDX analyses attributed of SEM were carried out with a JEOL Model JED-2300F operating at 13 kV.
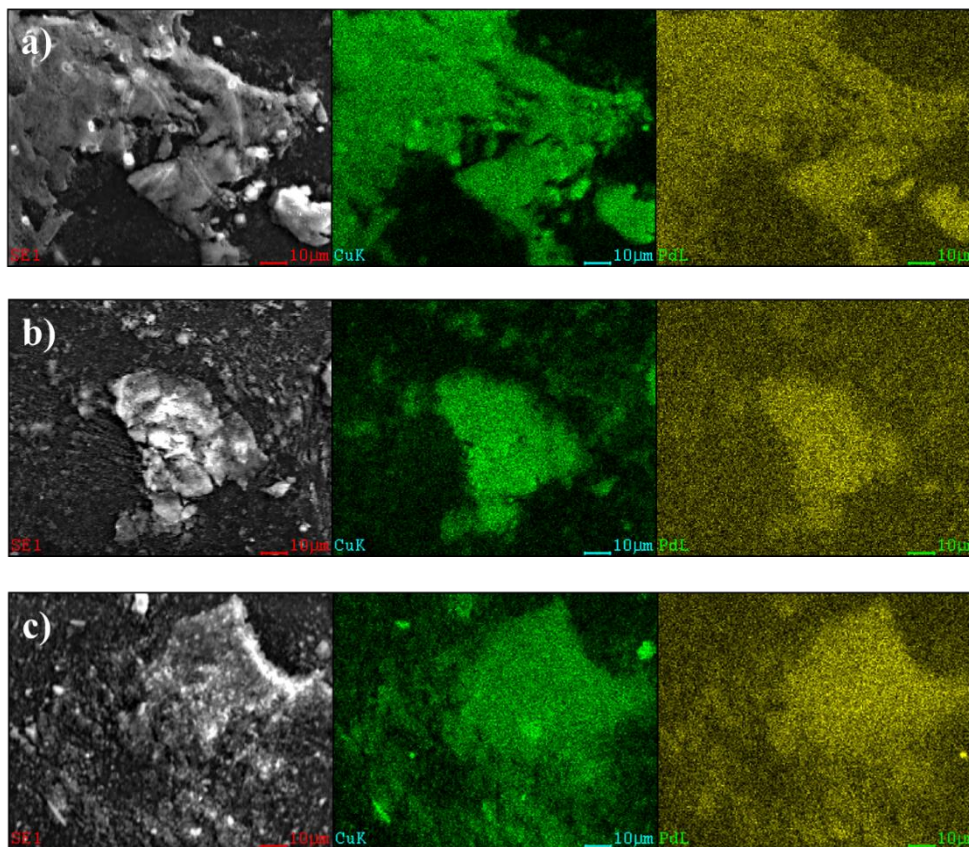

Fig. S6 SEM images (left) and EDX mapping of (a) **SIFSIX-1-CuPd-3**, (b) **SIFSIX-1-CuPd-5**, (c) **SIFSIX-1-CuPd-10** (middle: Cu, right: Pd).

Table S1 Feeding and obtained Pd atomic ratio by SEM/ EDX measurement.

Sample	Feeding [mol%]	Obtained [mol%]
SIFSIX-1-CuPd-3	3	3.56
SIFSIX-1-CuPd-5	5	4.46
SIFSIX-1-CuPd-10	10	9.69

Scanning Transmission Electron Microscopy (STEM) / EDX.

STEM measurements were performed with a JEOL Model JEM-2100F HK at 200 kV. The samples were heated at 120 °C in vacuum for 2 h. EDX analyses were operated at 200 kV.
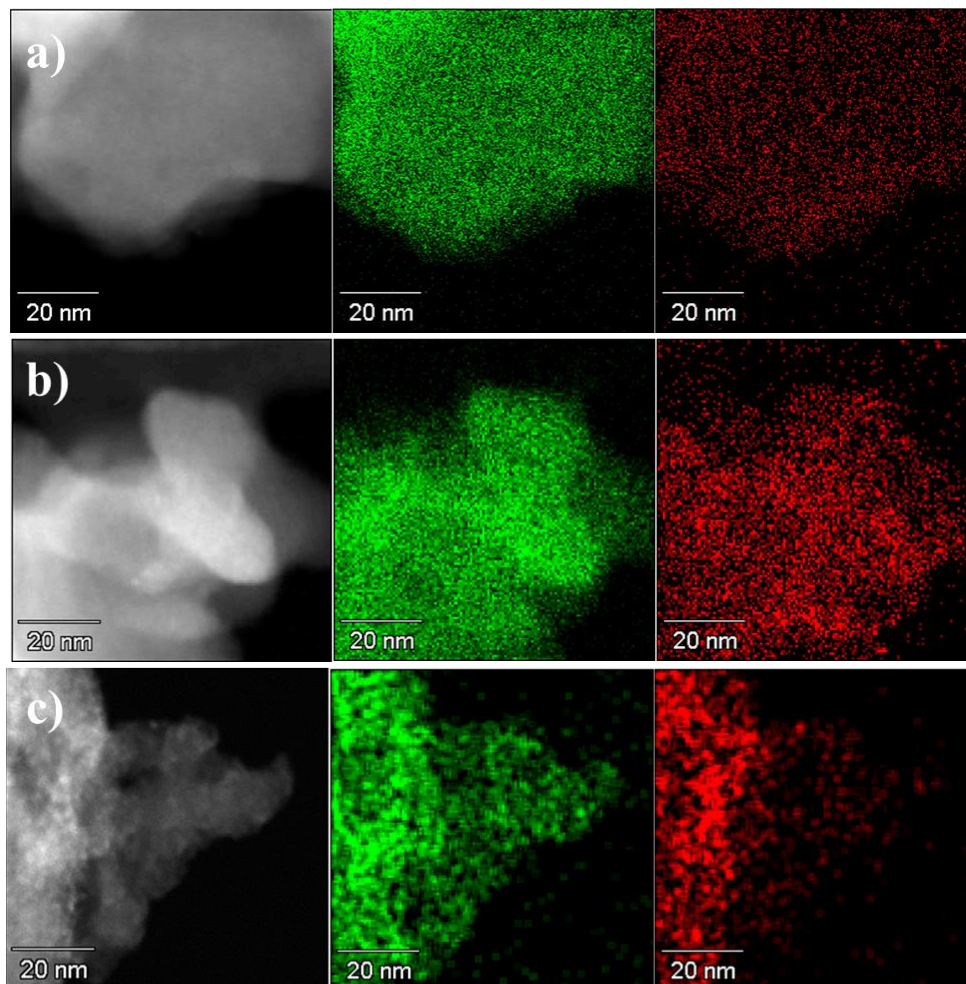

Fig. S7 STEM images (left) and EDX mapping of (a) **SIFSIX-1-CuPd-3**, (b) **SIFSIX-1-CuPd-5**, (c) **SIFSIX-1-CuPd-10** (middle: Cu, right: Pd).

Table S2 Feeding and obtained Pd atomic ratio by STEM/ EDX measurement.

Sample	Feeding [mol%]	Obtained [mol%]
SIFSIX-1-CuPd-3	3	5.24
SIFSIX-1-CuPd-5	5	6.50
SIFSIX-1-CuPd-10	10	8.77

Note: The difference of the Pd ratio from SEM/EDX should be derived from the local scanning area which is not representative of the entire chemical composition.

X-ray photoelectron spectroscopy (XPS) measurement.

XPS spectrum was measured by an ULVAC-PHI 5500 spectrometer with monochromatic Al Kα (1486.6 eV) source at 25.0 W. Before the measurement, the sample was embedded into the indium sheet and heated at 120 ˚C in vacuum for a day.
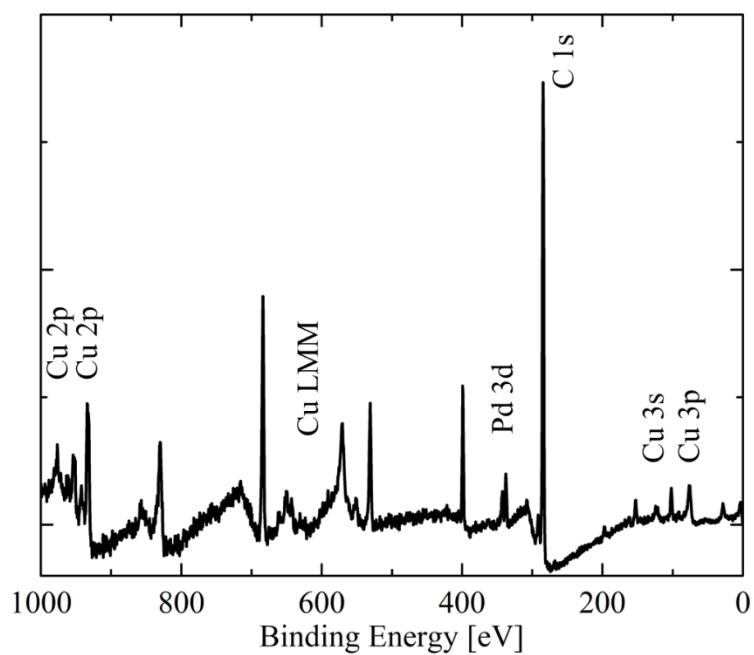
Fig. S8 XPS survey scan of **SIFSIX-1-CuPd-10**.

Thermogravimetric analysis (TGA).

TGA was performed using a Rigaku TP-EVO2 SL DyTG/DTA TypeJ under nitrogen stream scanning from 40 °C to 500 °C with the temperature ramp of 5 °C/min.
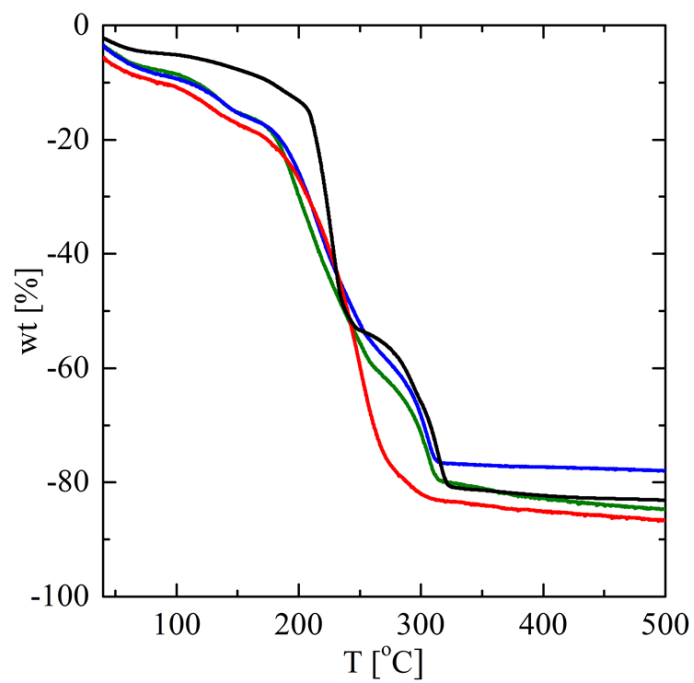

Fig. S9 TGA curves of **SIFSIX-1-Cu** and **SIFSIX-1-CuPd-n** (black: **SIFSIX-1-Cu**, green: **SIFSIX-1-CuPd-3**, blue: **SIFSIX-1-CuPd-5**, red: **SIFSIX-1-CuPd-10**).

Adsorption Measurement at 77 K.

The adsorption isotherms of N_2, O_2, and Ar at 77 K were obtained on a BELSORP-mini volumetric-adsorption instrument from microtrac-BEL, Inc. The measurement temperature (77 K) was maintained by liquid nitrogen. All measurements were carried out using the samples after activation under vacuum for 6 h at 120 °C.
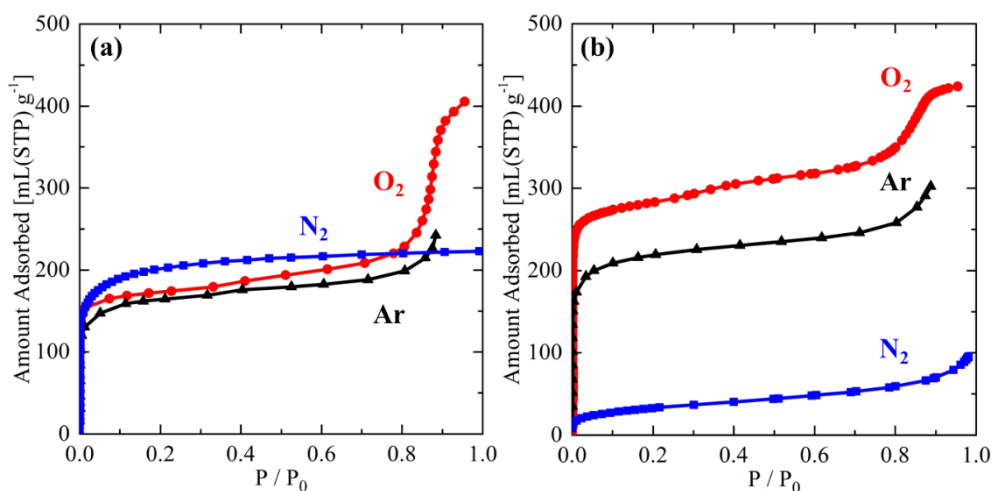

Fig. S10 Adsorption isotherms of N_2, O_2, and Ar for (a) **SIFSIX-1-Cu**, (b) **SIFSIX-1-CuPd-10** at 77 K. A steep increase in the adsorption amount of both samples at $P/P_0 = 0.8$ is possibly due to condensation or adsorption among nano-particles of the samples.
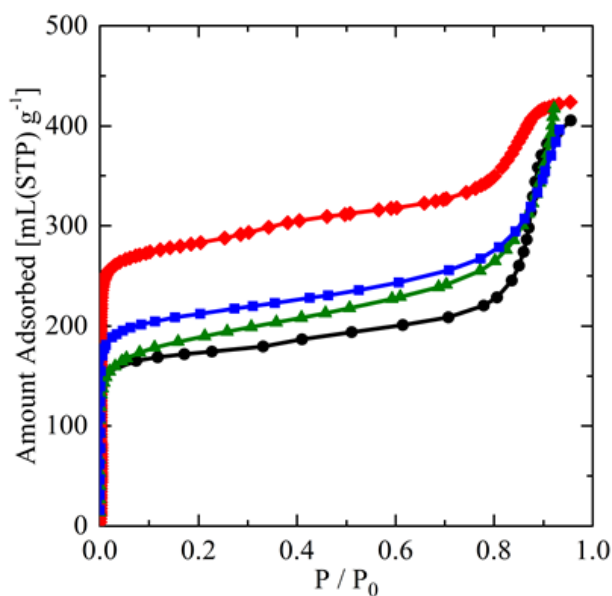

Fig. S11 Adsorption isotherms of O_2 at 77 K for **SIFSIX-1-Cu** and **SIFSIX-1-CuPd-n**.
(black: **SIFSIX-1-Cu**, green: **SIFSIX-1-CuPd-3**, blue: **SIFSIX-1-CuPd-5**, red: **SIFSIX-1-CuPd-10**)

Fig. S12 Adsorption isotherms of Ar at 77 K for **SIFSIX-1-Cu** and **SIFSIX-1-CuPd-n**.

(black: **SIFSIX-1-Cu**, green: **SIFSIX-1-CuPd-3**, blue: **SIFSIX-1-CuPd-5**, red: **SIFSIX-1-CuPd-10**)

Fig. S13 Adsorption isotherms of N_2 at 77 K for **SIFSIX-1-Cu** and **SIFSIX-1-CuPd-n**.

(black: **SIFSIX-1-Cu**, green: **SIFSIX-1-CuPd-3**, blue: **SIFSIX-1-CuPd-5**, red: **SIFSIX-1-CuPd-10**)
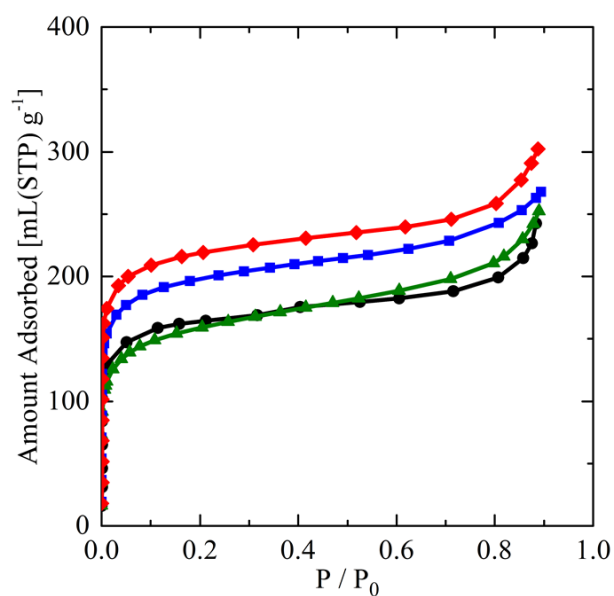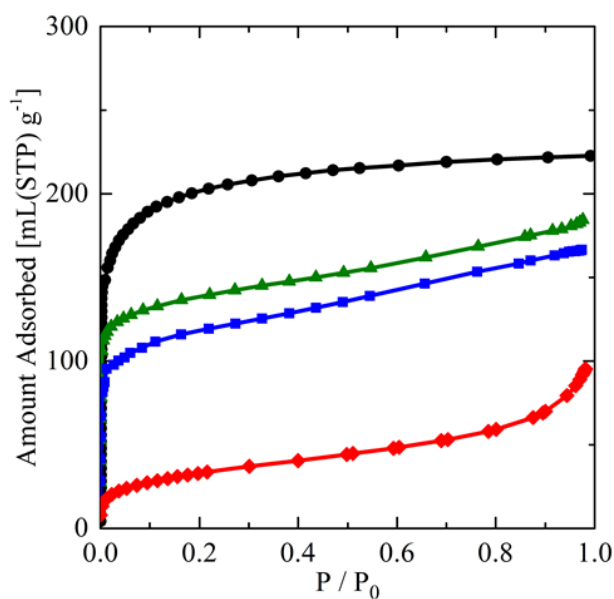
Density functional theory (DFT) calculation.

DFT calculations were carried out with M06 functional using the Gaussian 09.[2] The model structure was constructed using Pd^{2+} and four pyridine molecules (py) which coordinated to the central Pd^{2+}, i.e. $Pd(py)_4$ (Fig. S14). The basis sets were SDD for Pd and cc-pVTZ for the others in the all calculations. After the optimization of the $Pd(py)_4$, two oxygen molecules were disposed on the axial positions, i.e. $Pd(py)_4$–O_2 (Fig. 5a), and re-optimized. We performed DFT calculations for N_2 and Ar ($Pd(py)_4$-N_2 and $Pd(py)_4$-Ar) with the same procedure (Fig. 5b and 5c).

To understand effects of the OMS in the framework, we drew potential curves depending on the distance between Pd^{2+} ion and O_2 atoms and the angle of Pd-O-O. We calculated single point energy of $Pd(py)_4$-O_2 with various Pd-O distances (Fig. 6a) and Pd-O-O angles (Fig. 6b).
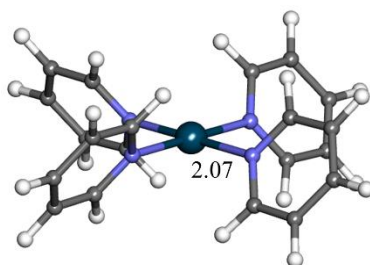

Fig. S14 The optimized structures of $Pd(py)_4$.

Reference

[1] S. D. Burd, S. Ma, J. A. Perman, B. J. Sikora, R. Q. Snurr, P. K. Thallapally, J. Tian, L. Wojtas, M. J. Zaworotko, *J. Am. Chem. Soc.*, 2012, **134**, 3663−3666.

[2] M. J. Frisch, G. W. Trucks, H. B. Schlegel, G. E. Scuseria, M. A. Robb, J. R. Cheeseman, G. Scalmani, V. Barone, G. A. Petersson, H. Nakatsuji, X. Li, M. Caricato, A. Marenich, J. Bloino, B. G. Janesko, R. Gomperts, B. Mennucci, H. P. Hratchian, J. V. Ortiz, A. F. Izmaylov, J. L. Sonnenberg, D. Williams–Young, F. Ding, F. Lipparini, F. Egidi, J. Goings, B. Peng, A. Petrone, T. Henderson, D. Ranasinghe, V. G. Zakrzewski, J. Gao, N. Rega, G. Zheng, W. Liang, M. Hada, M. Ehara, K. Toyota, R. Fukuda, J. Hasegawa, M. Ishida, T. Nakajima, Y. Honda, O. Kitao, H. Nakai, T. Vreven, K. Throssell, J. A. Montgomery Jr., J. E. Peralta, F. Ogliaro, M. Bearpark, J. J. Heyd, E. Brothers, K. N. Kudin, V. N. Staroverov, T. Keith, R. Kobayashi, J. Normand, K. Raghavachari, A. Rendell, J. C. Burant, S. S. Iyengar, J. Tomasi, M. Cossi, J. M. Millam, M. Klene, C. Adamo, R. Cammi, J. W. Ochterski, R. L. Martin, K. Morokuma, O. Farkas, J. B. Foresman and D. J. Fox, Gaussian 09, Revision A.02, Gaussian, Inc., Wallingford CT, 57 2016.